A Recursive Adaptive Method of Impulse Response Measurement with Constant SNR over Target Frequency Band

HIROKAZU OCHIAI AND YUTAKA KANEDA, *AES Member*
(kaneda@c.dendai.ac.jp)

Tokyo Denki University, Tokyo, Japan

A recursive adaptive method of impulse response measurement using a new measurement signal, i.e., a CSN-SS (constant-SNR swept-sine) signal is proposed. In the method, the spectrum of a measurement signal is shaped, adapting to not only the background noise spectrum but also the recursively estimated transfer function of the system itself. The measurement results show a constant SNR independent of frequency over the target frequency band, in which the system response can be properly identified.

0 INTRODUCTION

Impulse response is one of the most important characteristics of acoustic systems. Since most acoustic systems can be considered to be linear systems, the output of acoustic systems is represented as the convolution of an input signal and the impulse response. On the basis of this property, impulse response is widely used in the simulation of acoustic systems. Moreover, the frequency response (transfer function) of an acoustic system can be obtained by applying a Fourier transform to the impulse response. Frequency response is the most basic characteristic of acoustic equipment such as loudspeakers, microphones, and various acoustic systems. In architectural acoustics, various characteristics of rooms, such as reverberation time, can be derived from the impulse response [1].

Impulse response is defined as the output obtained when an impulse signal is input to a system. However, we cannot obtain an impulse response with a high signal-to-noise ratio (SNR) because the practical impulse signal has a low energy. Therefore, maximum-length-sequence (MLS) signals [2]-[6] and swept sine (SS) signals [7]-[9], both of which have high energy, have been used as measurement signals (signals input to a target acoustic system for the measurement of impulse response).

MLS signals are binary white noise composed of –1 and 1, and can be synthesized using simple hardware. The cost of the calculation required to obtain the impulse response from the MLS response is small. On the other hand, SS signals are sine signals whose frequency monotonically increases (or decreases) with time. Although several sweeping methods have been proposed to obtain SS signals, the most basic method is linear sweeping, in which the frequency of the sine signal increases proportionally with time. The linear SS signals are also called time-stretched pulse (TSP) signals [7], [8] and have been widely used because of their simple structure.

The problems in impulse response measurement are (a) measurement errors due to the nonlinearity of the system to be measured and (b) those due to noise (acoustic and electric noise) mixed into the response signal during measurement. Differences among various measurement signals are characterized by the effect of these errors.

SS signals with a frequency that exponentially increases with time are called exponential swept sine (ESS) signals; they are also called logarithmic SS (Log-SS) signals because their logarithmic frequency increases proportionally with time. Recently, ESS signals have been widely used because of their desirable feature that the harmonic distortion components generated by the nonlinearity of a system can be separated and removed [10]-[13]. However, the effect of errors due to nonlinearity in a linear response cannot be removed even by using ESS signals [14], [15]. Therefore, the errors due to nonlinearity still remain as a problem, and we should avoid excessively high signal amplitudes.

Stationary noise present in rooms, such as the noise from air conditioners, has many low-frequency components. The effect of such acoustic noise can be reduced when ESS signals are used because their energy is high in the low-frequency region; thus, the SNR in the low-frequency region can be increased. On the other hand, the SNR in the high-frequency region decreases when using ESS signals. To solve this problem, the use of signals that are logarithmically swept in the low-frequency region and linearly

swept in the high-frequency region has been proposed [16]. However, these signals can increase the SNR only in the low-frequency region and their optimality is not assured.

If the power spectrum of the stationary noise can be measured in advance, a more sophisticated measurement result can be obtained by adapting a measurement signal spectrum to the noise spectrum. When the signal power spectrum is determined so that it is proportional to that of noise, the noise power spectrum is whitened [17]. On the other hand, Moriya and Kaneda proposed another SS signal by which the energy of noise components included in measurement results is minimized, i.e., a minimum-noise SS (MN-SS) signal, using the known power spectrum of noise [18], [19]. However, it is still difficult to observe the characteristic of a frequency response with low response levels, even when the noise energy is reduced by these methods.

In this study we propose the concept of an SS signal that maintains a constant SNR regardless of the frequency, i.e., a constant-SNR SS (CSN-SS) signal [20], [21]. Here, the SNR refers to the power ratio of the frequency response of a system to the noise components included in the measurement result of the frequency response. We also propose a recursive measurement algorithm to realize the constant-SNR measurement. In the measurement results obtained using CSN-SS signals, a constant SNR can be achieved even in the frequency band of an unknown system in which response levels are small, enabling the observation of the characteristics in this frequency band.

In Section 1, the problems of conventional measurement methods are pointed out. We explain our new measurement method to solve these problems in Section 2. The validity of the proposed method is experimentally verified in Section 3, and the conclusions of this study are described in Section 4.

1 PROBLEMS IN CONVENTIONAL IMPULSE RESPONSE MEASUREMENT METHODS

1.1 Principle of Measurement

In this study we focus on the measurement of the frequency response $H(\omega)$ of a linear system, which is the frequency domain representation of the impulse response $h(t)$. Fig. 1(a) shows the principle of frequency response measurement for an unknown system. For simplicity, the variable ω is omitted from the figure. First, a measurement signal with a spectrum $S(\omega)$ is input to an unknown system with a frequency response $H(\omega)$. The output of the unknown system is $H(\omega) \cdot S(\omega)$. When this output signal is filtered through an inverse filter $1/S(\omega)$, $H(\omega)$ of the unknown system can be obtained. The impulse response $h(t)$ can be obtained by applying an inverse Fourier transform to $H(\omega)$.

When a measurement based on the above principle is carried out in an actual environment, noise $N(\omega)$ (including ambient and electric noise) is added to the system output $H(\omega) \cdot S(\omega)$, as shown in Fig. 1(b), resulting in the measured signal $H(\omega) \cdot S(\omega) + N(\omega)$. When this signal is filtered through an inverse filter, the measurement result (estimated $H(\omega)$) is obtained as

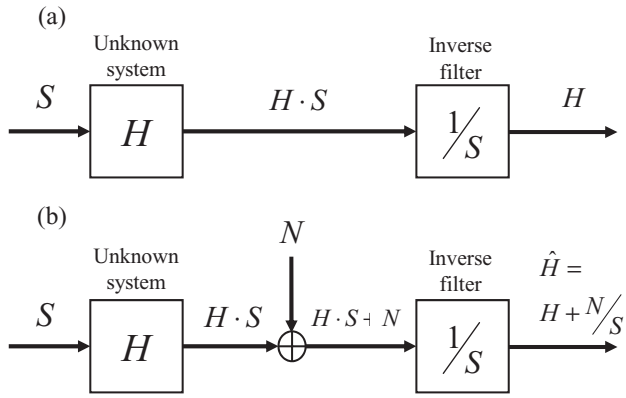

Fig. 1. Measurement principle of frequency response H. (a) Ideal system. (b) Actual measurement system into which noise is added.

$$\hat{H}(\omega) = H(\omega) + N(\omega)/S(\omega). \tag{1}$$

Thus, noise components with the spectrum $N(\omega)/S(\omega)$ are included in the measurement result.

1.2 Measurement Signals and Noise Components

The power spectrum of noise components included in the measurement result $\hat{H}(\omega)$ is

$$E[|N(\omega)/S(\omega)|^2] = P_N(\omega)/|S(\omega)|^2, \tag{2}$$

where $E[\bullet]$ represents expectation and $P_N(\omega)$ is the power spectrum of the added noise.

$$P_N(\omega) = E[|N(\omega)|^2] \tag{3}$$

Eq. (2) indicates that the noise components depend on the power spectrum of the measurement signal, i.e., $|S(\omega)|^2$. Typical measurement signals, such as TSP signals and MLS signals have a flat spectrum ($|S(\omega)|^2 = const.$). Upon substituting this into Eq. (2), the power spectrum of the noise components included in the measurement results obtained using these signals becomes proportional to that of added noise, i.e., $P_N(\omega)$.

Fig. 2 shows a schematic diagram of the power spectrum of noise components included in the measurement result obtained using a signal with a flat spectrum. In this figure, the bold line represents the power response of an unknown system $|H(\omega)|^2$, and the gray area represents the power spectrum of noise components. As indicated by the dotted circles, the response is hidden by noise (a) in a frequency band where the noise components are large and (b) in a frequency band where the response levels of the system are small, which makes it difficult to observe the response characteristics.

To overcome this problem, Moriya and Kaneda proposed the MN-SS signal, as described in Section 0 [18], [19]. The MN-SS signal has a power spectrum proportional to the root square of the power spectrum of noise, i.e., $|S(\omega)|^2 \propto \sqrt{P_N(\omega)}$, and minimizes the noise components. On the other hand, Weinzierl et al. whitened the noise components

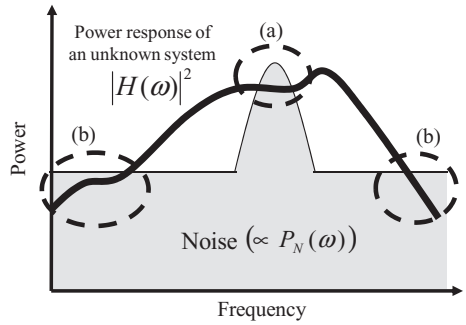

Fig. 2. Power spectrum of noise components (gray area) included in measurement result obtained using signal with flat spectrum. The power spectrum of noise components is proportional to that of the added noise, $P_N(\omega)$. Dotted circles indicate frequency bands where the desired response is poorly observable.

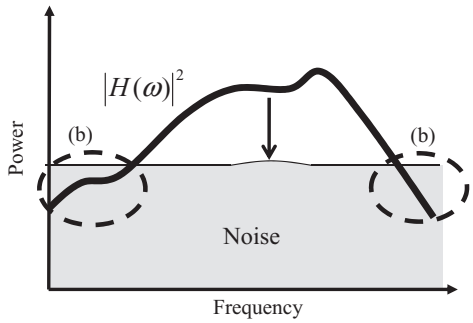

Fig. 3. Power spectrum of noise components (gray area) included in measurement result obtained using MN-SS signal. Large noise components are reduced.

by matching the power spectrum of a measurement signal to that of the noise, i.e., $|S(\omega)|^2 \propto P_N(\omega)$ [17]. When these measurement signals were used, large noise components were reduced and the effect of noise was alleviated, as shown in Fig. 3. However, the frequency response was still affected by noise components in the frequency band where the power response $|H(\omega)|^2$ was small, as indicated by the dotted circles in Fig. 3, and this has remained a problem.

In this study we propose a CSN-SS signal, a measurement signal that maintains a constant SNR in the measurement result regardless of the frequency, as shown in Fig. 4. The CSN-SS signal shapes the power spectrum of noise components into the power response $|H(\omega)|^2$ of the system. Although the measurement result includes a frequency band in which the noise energy is higher than that in Fig. 3, the noise energy is lower in frequency bands where the power response $|H(\omega)|^2$ is small. Thus, the CSN-SS signal makes it possible to observe the characteristics of the frequency response in a wider frequency band with equal quality.

2 MEASUREMENT METHOD USING CSN-SS SIGNAL

2.1 Spectrum of CSN-SS Signal

From Eqs. (1) and (2), the SNR of the measurement result $\hat{H}(\omega)$ for each frequency component is the ratio of $|H(\omega)|^2$ to $P_N(\omega)/|S(\omega)|^2$. Assuming that the SNR is a constant C^2 that is independent of frequency, the following relationship holds.

$$SNR(\omega) = \frac{|H(\omega)|^2}{P_N(\omega)/|S(\omega)|^2} = C^2 \tag{4}$$

By solving Eq. (4) for $|S(\omega)|^2$, we obtain

$$|S(\omega)|^2 = C^2 \cdot P_N(\omega)/|H(\omega)|^2. \tag{5}$$

Therefore, when a measurement signal has a power spectrum of $|S(\omega)|^2$ given by Eq. (5), the SNR can be maintained constant regardless of frequency.

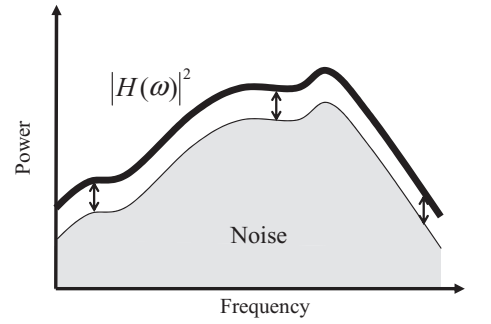

Fig. 4. Power spectrum of noise components (gray area) included in measurement result obtained using CSN-SS signal. The power spectrum of the noise components is shaped into the power response $|H(\omega)|^2$. Thus, the SN ratio becomes constant regardless of the frequency, enabling the observation of the response in a wider frequency band.

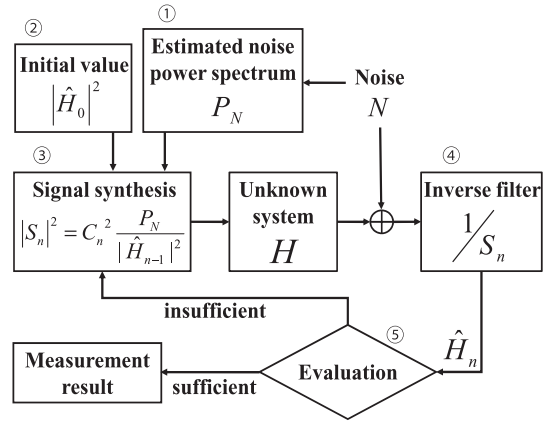

Fig. 5. Block diagram of proposed measurement algorithm.

2.2 Measurement Algorithm

When the measurement noise is assumed to be stationary, it is possible to estimate $P_N(\omega)$ in Eq. (5) in advance. However, the power response of the system to be measured, $|H(\omega)|^2$, is unknown before measurement. In our proposed method, $|S(\omega)|^2$ is calculated from Eq. (5) using the estimated $H(\omega)$, i.e., $\hat{H}(\omega)$. The measurement is repeated iteratively using $\hat{H}(\omega)$ to increase measurement accuracy.

Fig. 5 shows the measurement algorithm in our proposed method. This algorithm is explained below with numbers corresponding to those in Fig. 5. Here, the signal and

spectrum are assumed to be those of a discrete system, and the discrete frequency number is denoted as k. The subscript n in the figure represents the number of iterations.

1) The noise power spectrum, $P_N(k)$ (variable k is omitted in the figure), of a target frequency band is estimated. One way to estimate $P_N(k)$ is to apply a discrete Fourier transform (DFT) to the autocorrelation function of the measured noise.

2) An initial estimate of $H(k)$, which is denoted as $\hat{H}_0(k)$, is given. For example, when $H(k)$ can be roughly estimated, the estimated characteristic should be given; otherwise, $\hat{H}_0(k) = 1$, which whitens noise components in the measurement result, or $|\hat{H}_0(k)|^2 = \sqrt{P_N(k)}$, which minimizes noise components.

3) A measurement signal with a power spectrum given by

$$|S_n(k)|^2 = C_n^2 \cdot P_N(k)/|\hat{H}_{n-1}(k)|^2 \tag{6}$$

is synthesized, where $n = 1$ for the first iteration. Outside of the target frequency band, $|S_n(k)|^2$ is set to a small constant value.

When C_n^2, which is a constant that controls the signal amplitude, increases, the SNR also increases. In practice, however, nonlinear distortion is induced by, for example, a loudspeaker when the amplitude of the measurement signal is excessively increased; the amplitude of the measurement signal should thus be restricted to a certain level. In this method, the signal energy (the sum of the power spectra over the frequencies) is restricted to a constant value E_s as follows:

$$\sum_{k=0}^{L-1} |S_n(k)|^2 = E_S. \tag{7}$$

Here, L represents the length of the DFT (= signal length). By substituting Eq. (6) into Eq. (7), we obtain

$$C_n^2 \cdot \sum_{k=0}^{L-1} \left\{ P_N(k) \Big/ \left|\hat{H}_{n-1}(k)\right|^2 \right\} = E_S. \tag{8}$$

Therefore, C_n^2 is given by

$$C_n^2 = E_S \Bigg/ \sum_{k=0}^{L-1} \left\{ P_N(k) \Big/ \left|\hat{H}_{n-1}(k)\right|^2 \right\}. \tag{9}$$

Although there are several possible signals with a power spectrum given by Eq. (6), we adopt an SS signal with constant amplitude because of its small crest factor. The details of the method used to synthesize an SS signal are explained in Appendix 1.

4) The synthesized measurement signal is input to an unknown system, and the observed signal is filtered through an inverse filter to obtain the measurement result (estimated response) $\hat{H}_n(k)$. Here, the circular convolution of the input signal $s_n(t)$ and the impulse response in the unknown system must be assumed so that $1/S_n(k)$ acts as the inverse filter of the discrete system. To this end, $s_n(t)$ for two periods is input and the output signal in the second period is extracted.

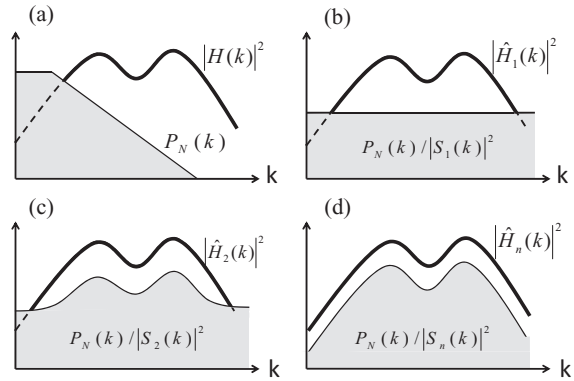

Fig. 6. Model figures showing convergence process. (a) Power response of unknown system $|H(k)|^2$ and power spectrum of added noise $P_N(k)$. (b) Measurement result after first iteration with $\hat{H}_0(k) = 1$. Spectrum of noise components (gray area) is whitened. (c) Measurement result after second iteration. The SN ratio becomes constant in the frequency band where the SN ratio is high in (b). (d) Measurement result after nth iteration. SN ratio becomes almost constant regardless of the frequency.

The extracted signal is subjected to a DFT, and the result is multiplied by the inverse filter characteristic $1/S_n(k)$. Here, attention must be paid into the division by the very small $S_n(k)$. Regularization, that is, adding a small quantity to the denominator, prevents the reciprocal from taking an extremely large value.

Then, the result is subjected to an inverse DFT to obtain a system impulse response of length L. The impulse response is windowed for its duration to improve the SNR. Finally, the windowed impulse response is zero-padded to be of length L and subjected to a DFT to obtain $\hat{H}_n(k)$.

5) Whether a constant SNR characteristic is achieved satisfactorily is evaluated by calculating the SNR in each frequency band. When it is evaluated to be insufficient, steps (3)–(5) are repeated using $\hat{H}_n(k)$. When it is evaluated to be satisfactory, the above iteration is ended and the obtained result is considered to be the final measurement result.

2.3 Convergence Characteristics of Algorithm

When the proposed algorithm is used, the following measurement results are obtained depending on the number of iterations.

- First iteration
  When the initial $\hat{H}_n(k)$ is 1, i.e., $\hat{H}_0(k) = 1$, we obtain $|S_1(k)|^2 = C_1^2 P_N(k)$. Therefore, the power spectrum of noise components included in the first estimation, $P_N(k)/|S_1(k)|^2$, is whitened. Fig. 6 shows schematic diagrams of the convergence process. Fig. 6(a) shows the power response of an unknown system $|H(k)|^2$ and the power spectrum of the added noise $P_N(k)$. Fig. 6(b) shows the first measurement result, where the power spectrum of noise components (gray area) is whitened.
- Second iteration

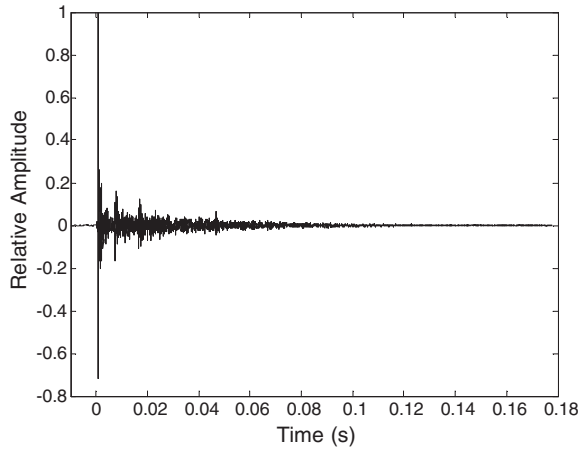

Fig. 7. Room impulse response measured when major noise sources were turned off.

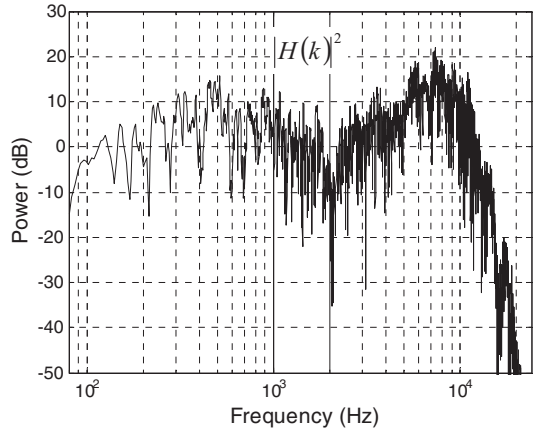

Fig. 8. Room frequency response measured when major noise sources were turned off.

In the frequency band where SNR higher than 0 dB was obtained in the first measurement, the SNR becomes almost constant in the second measurement result, $|\hat{H}_2(k)|^2$ (Fig. 6(c)). In this frequency band, the SNR is C_2^2.

- Third and subsequent iterations
  In the frequency band where the SNR becomes constant in $\hat{H}_2(k)$, the SNR also remains constant in the third and subsequent measurements. The frequency band with the constant SNR is widened with increasing number of iterations. In contrast, the SNR decreases with increasing width of this frequency band (Fig. 6(d)). The constant SNR can be expected to be C_n^2 before the nth measurement.

Although the above results were experimentally obtained, some of them are proved in Appendix 2.

3 EXPERIMENTS

3.1 Measurement of Room Impulse Response

To verify the validity of the proposed method in an actual environment, we measured the impulse response of a small laboratory room. The room volume was about 60 m^3 (7 × 3.2 × 2.7 m) and its reverberation time was 300 ms. The environmental noise was the stationary mixture noise of an air conditioner, PC fans, and machines. The sampling frequency was 48 kHz and the measurement signal duration was 2^{15} samples (about 0.7 second). A full-range loudspeaker was used for the measurement. The distance between the loudspeaker and the microphone was about 2 m. Figs. 7 and 8 show the room impulse response and its frequency response, which were measured when major noise sources were turned off. The target frequency band was set in the range from 80 Hz to 16 kHz.

3.2 Experimental Results

First, the measurement was carried out using a TSP signal (an SS signal with a white spectrum, i.e., $|S(k)|^2 =$ const.). Fig. 9 shows the measured frequency (power) response $|\hat{H}(k)|^2$, and the noise components included in the measurement result. In the figure, the thin line represents the frequency response, $|\hat{H}(k)|^2$, and the bold line represents the noise components. The noise components were calculated from the received sound signal that contains only room noise.

As explained in Section 1.2, the spectrum of the noise components obtained using a TSP signal is in agreement with that of room noise. Fig. 9 indicates that room noise has a higher power at lower frequencies and that the measured frequency response is degraded in the low-frequency band. Fig. 10 shows the SNR in the 1/3 octave frequency band corresponding to Fig. 9. This figure shows that below 200 Hz, SNR is below 10 dB.

Next, the measurement results obtained by the proposed method are demonstrated. In the first measurement, $|\hat{H}_0(k)|^2 = 1$ was assumed, and from Eq. (6), a measurement signal with a power spectrum proportional to that of room noise $P_N(k)$ was used. Fig. 11 shows the measurement result, which indicates that the noise components are whitened, as explained in Section 2.3. Because the noise components are whitened, the SNR is improved in the low-frequency band where the original noise power is high. However, in the frequency range below 100 Hz, the SNR is still low. In addition, in the high-frequency band above 13 kHz, in which the response level of $|\hat{H}_1(k)|^2$ is small, the SNR becomes worse. Thus, in those frequency bands, the measurement result, $|\hat{H}_1(k)|^2$, is affected by noise and fluctuates. Fig. 12 shows the 1/3 octave band SNR corresponding to Fig. 11. We can see the SNR is below 10 dB in those frequency bands.

Fig. 13 shows the second measurement result obtained using a measurement signal, $S_2(k)$, with a power spectrum calculated from $\hat{H}_1(k)$ using Eqs. (6) and (9). In the figure, noise components were shaped proportionally to the power response $|\hat{H}_2(k)|^2$ at almost all frequencies. This means a constant SNR was realized.

Comparing Fig. 13 with Fig. 9, which is the measurement result obtained by using the conventional signal that has a white spectrum, we found that the frequency response becomes clearly observable in the low-frequency band. Comparing Fig. 13 with Fig. 11, which is the first measurement

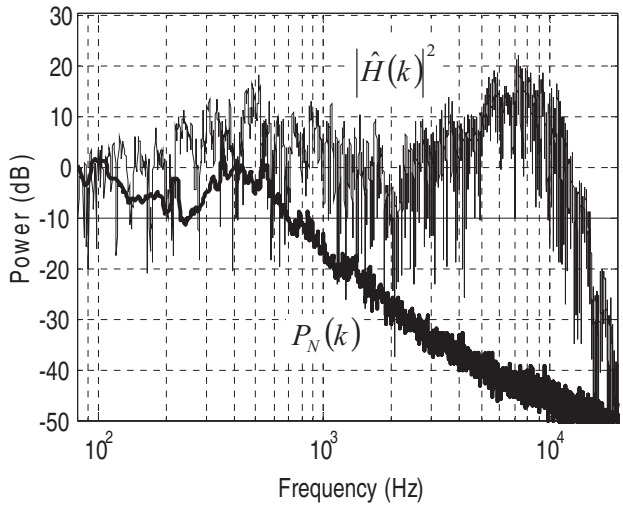

Fig. 9. Measurement result obtained using TSP signal and noise components included in the result.

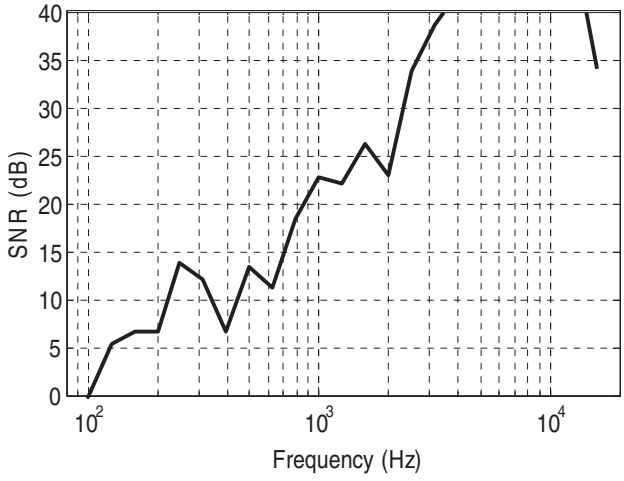

Fig. 10. 1/3 octave band SNR corresponding to Fig. 9.

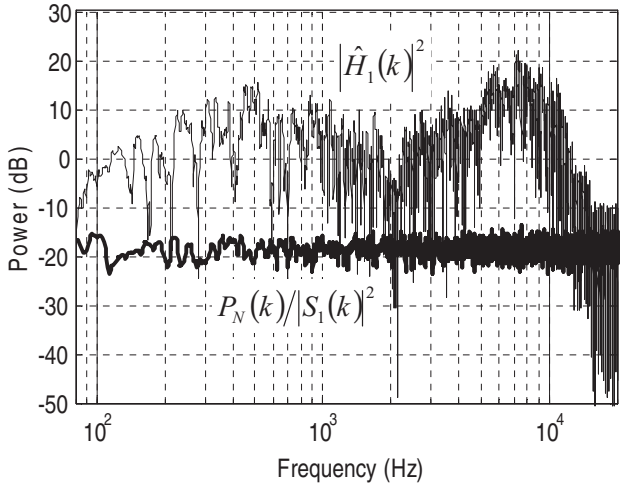

Fig. 11. Result of first measurement by proposed method. Noise components are whitened.

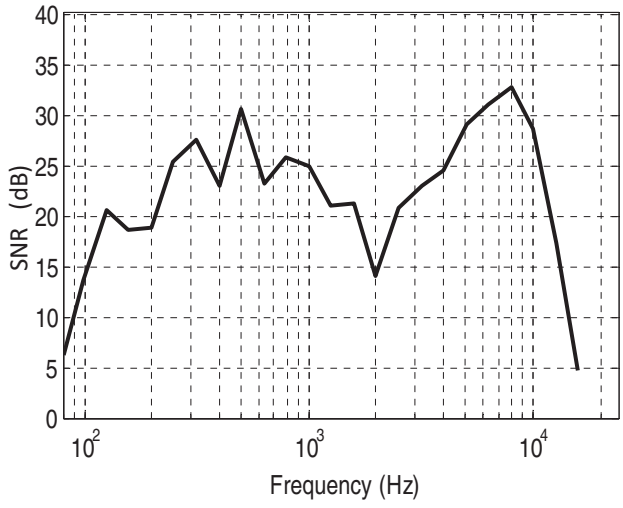

Fig. 12. 1/3 octave band SNR corresponding to Fig. 11.

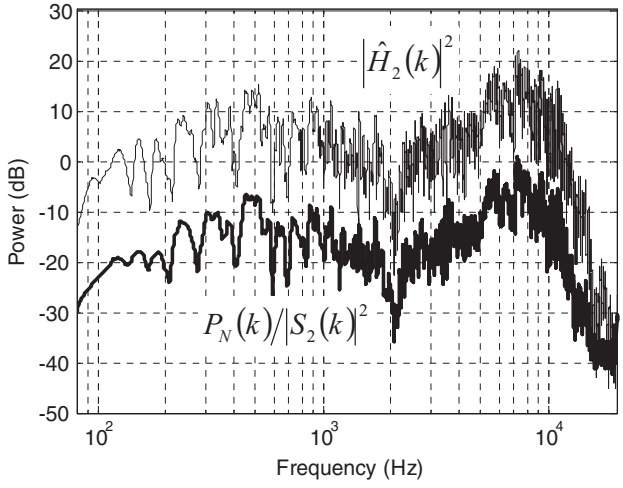

Fig. 13. Result of second measurement by proposed method. An almost constant SNR is realized over the target frequency band, 80 Hz–16 kHz.

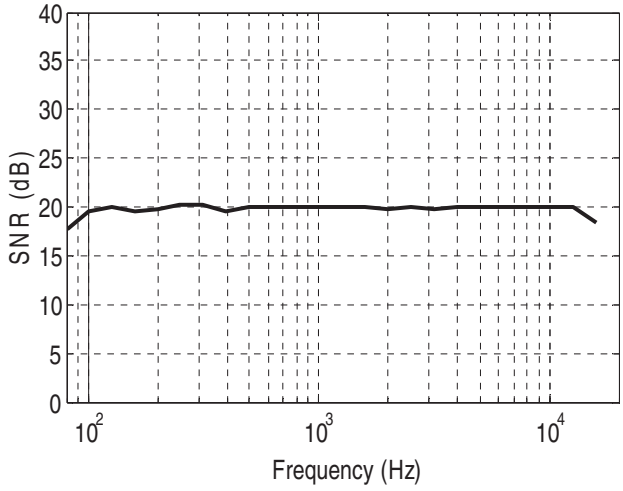

Fig. 14. 1/3 octave band SNR corresponding to Fig. 13.

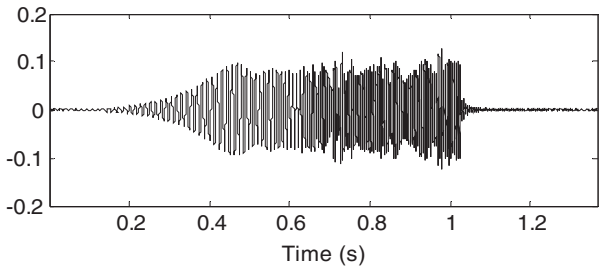

Fig. 15. Waveform of CSN-SS signal used in the second measurement.

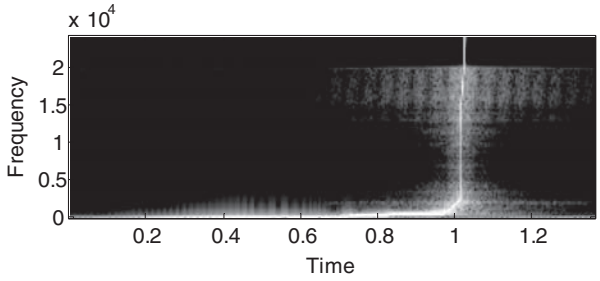

Fig. 16. Time-frequency characteristics of CSN-SS signal used in the second measurement.

result obtained by the proposed method but at the same time the result obtained by the conventional noise-whitening signal, we found that the frequency response is less affected by the noise in the low-frequency and high-frequency bands. Fig. 14 show the 1/3 octave band SNR corresponding to Fig. 13. From the figure, it is observed that the SNR is almost constant at 20 dB over the target frequency band. Thus, the constant SNR characteristic of the proposed method was verified.

Fig. 15 shows the time waveform of the CSN-SS signal used in the second measurement. Fig. 16 shows the time-frequency characteristics (corresponding to the group delay characteristics) of the CSN-SS signal in Fig. 15. The CSN-SS signal takes a long time to sweep the low-frequency band where the SNR is very low. In contrast, it takes a short time to sweep the high-frequency band where the SNR is high.

To simply improve SNR, we can adopt another method, an "averaging method." However, the averaging method takes time. Let us assume we need an SNR of more than 17 dB over the target frequency band. As seen in Fig. 14, the proposed method achieved this in two measurements. However, Figs. 10 or 12 show that for the results derived from the conventional signals, their SNR should be improved by more than 10 dB in low-SNR frequency bands. To achieve this, more than 10 repetitions of measurements by the averaging method are required.

4 CONCLUSIONS

In this study we proposed a new recursive adaptive method of impulse response measurement using a new measurement signal, i.e., a CSN-SS (constant-SNR swept-sine) signal. The spectrum of the CSN-SS signal is determined to adapt itself to the noise power spectrum and the frequency response of a system. The measurement result of the frequency response of the unknown system by the proposed method has a constant SNR in the target frequency band.

We first discussed the spectrum of the measurement signal required to maintain the SNR in a measurement result at a constant value regardless of the frequency using the noise power spectrum, $P_N(\omega)$, and the frequency response of the system to be measured, $H(\omega)$. When the noise is stationary, it is possible to estimate $P_N(\omega)$ in advance. However, $H(\omega)$ is generally unknown before its measurement. Then, we proposed an iterative measurement algorithm that recursively estimates the frequency response, $H(\omega)$.

To verify the validity of our proposed method, we measured the room impulse response in a noisy environment and calculated a room frequency response. The experimental result showed a frequency response with an almost constant SNR was obtained by two iterations of measurements. As a result, we confirmed that our method enabled the observation of the frequency response with less influence of the noise in frequency bands where the original NSR was low than when using conventional measurement signals.

Thus, we experimentally confirmed the constant SNR characteristic by the proposed method. The constant SNR characteristic ensures the equal quality of measured frequency response over the target frequency band. In addition to that, the constant SNR characteristic is expected to be useful in reverberation time measurement because it provides a reverberation curve of the constant SNR quality independent of the frequency.

The signal that achieves a constant SNR characteristic is not restricted to the SS signal. We can also choose other signals such as pseudo random noise that has the same power spectrum as the CSN-SS signal. Performance studies of other types of signals that have a CSN spectrum are left for future work.

5 ACKNOWLEDGMENT

The authors would like to thank Professor Tatsuya Hirahara of Toyama Prefectural University, Japan, for the discussion that motivated us to start this work.

6 REFERENCES

[1] H. Kuttruff, *Room Acoustics* (London, Elsevier Science Publishers, 1973), pp. 231–243.

[2] J. Borish, "An Efficient Algorithm for Measuring the Impulse Response Using Pseudorandom Noise," *J. Audio Eng. Soc.*, vol. 31, pp. 478–488 (1983 July/Aug.).

[3] J. Borish, "Self-Contained Crosscorrelation Program for Maximum-Length Sequences," *J. Audio Eng. Soc.*, vol. 33, pp. 888–891 (1985 Nov.).

[4] D. D. Rife and J. Vanderkooy, "Transfer-Function Measurement with Maximum-Length Sequences," *J. Audio Eng. Soc.*, vol. 37, pp. 419–444 (1989 June).

[5] J. Vanderkooy, "Aspects of MLS Measuring Systems," *J. Audio Eng. Soc.*, vol. 42, pp. 219–231 (1994 Apr.).

[6] C. Dunn and M. O. Hawksford, "Distortion Immunity of MLS-Derived Impulse Response Measurements," *J. Audio Eng. Soc.*, vol. 41, pp. 314–335 (1993 May).

[7] N. Aoshima, "Computer-Generated Pulse Signal Applied for Sound Measurement," *J. Acoust. Soc. Am.*, vol. 69, no. 5, pp. 1484–1488 (1981 May).

[8] Y. Suzuki, F. Asano, H. Kim, and T. Sone, "An Optimum Computer-Generated Pulse Signal Suitable for the Measurement of Very Long Impulse Response," *J. Acoust. Soc. Am.*, vol. 97, no. 2, pp. 1119–1123 (1995 Feb.).

[9] S. Muller and P. Massarani, "Transfer-Function Measurement with Sweeps," *J. Audio Eng. Soc.*, vol. 49, pp. 443–471 (2001 June).

[10] T. Fujimoto, "A Study of TSP Signal Getting Higher SNR at Low Frequency Bands," *Proc. Autumn Meet. Acoust. Soc. Jpn.*, pp. 433–434 (1999 Sept.) [in Japanese].

[11] A. Farina, "Simultaneous Measurement of Impulse Response and Distortion with a Swept-Sine Technique," presented at the *108th Convention* of the Audio Engineering Society (2000 Feb.), convention paper 5093.

[12] A. Farina, "Advancements in Impulse Response Measurements by Sine Sweeps," presented at the *122nd Convention* of the Audio Engineering Society (2007 May), convention paper 7121.

[13] G. B. Stan, J. J. Embrechts and D. Archambeau, "Comparison of Different Impulse Response Measurement Techniques," *J. Audio Eng. Soc.*, vol. 50, pp. 249–262 (2002 Apr.).

[14] N. Moriya and Y. Kaneda, "Study of Harmonic Distortion on Impulse Response Measurement with Logarithmic Time Stretched Pulse," *Acoust. Sci. & Tech.*, vol. 26, no. 5, pp. 462–464 (2005 Sept.).

[15] A. Torras-Rosell and F. Jacobsen, "A New Interpretation of Distortion Artifacts in Sweep Measurements," *J. Audio Eng. Soc.*, vol. 59, pp. 283–289 (2011 May).

[16] M. Morise, T. Irino, H. Banno and H. Kawahara, "Warped-TSP: An Acoustic Measurement Signal Robust to Background Noise and Harmonic Distortion," *Electronics and Communications in Japan* (Part III: Fundamental Electronic Science), vol. 90, no. 4, pp. 18–26 (2007 April).

[17] S. Weinzierl, A. Giese, and A. Lindau, "Generalized Multiple Sweep Measurement," presented at the *126th Convention of the Audio Engineering Society*(2009 May), convention paper 7767 .

[18] N. Moriya and Y. Kaneda, "Impulse Response Measurement that Maximizes Signal-to-Noise Ratio against Ambient Noise," *Acoust. Sci. & Tech.*, vol. 28, no. 1, pp. 43–45 (2007 Jan.).

[19] N. Moriya and Y. Kaneda, "Optimum Signal for Impulse Response Measurement that Minimizes Error Caused by Ambient Noise," *J. Acoust. Soc. Jpn.*, vol. 64, no. 12, pp. 695–701 (2008 Dec.) [in Japanese].

[20] H. Ochiai and Y. Kaneda, "A Study of Impulse Response Measurement with Constant SN Ratio over All Frequency Bands," in *Proc. Spring Meet. Acoust. Soc. Jpn.*, pp. 879–880 (2010 Mar.) [in Japanese].

[21] H. Ochiai and Y. Kaneda, "Impulse Response Measurement with Constant Signal-to-Noise Ratio over a Wide Frequency Range," *Acoust. Sci. & Tech.*, vol. 32, no. 2, pp. 76–78 (2011 Mar.).

APPENDIX 1

METHOD OF SYNTHESIZING SS SIGNAL

A method of synthesizing an SS signal that has the desired power spectrum is explained below.

When the phase characteristic of a signal is differentiated with respect to angular frequency, a group delay characteristic is obtained. For an SS signal with a constant amplitude, the power spectrum of the SS signal is obtained when the group delay characteristic is differentiated with respect to frequency. In contrast, the group delay characteristic of the SS signal with the desired power spectrum can be obtained by integrating the desired power spectrum over frequency [9].

Therefore, the group delay characteristic of a signal with the desired power spectrum $|S(k)|^2$, i.e., $D(k)$, is obtained by integrating $|S(k)|^2$ over frequency as

$$D(k) = \alpha_1 \cdot \left\{ \sum_{i=0}^{k} |S(i)|^2 - |S(0)|^2 \right\}, \tag{10}$$

where i and k ($i, k = 0, 1, 2, \ldots, L/2, 0 \leq i \leq k$) are the discrete frequency numbers and L is the length of the DFT (and also the length of the SS signal). Because a discrete system is assumed, this integration over frequency is expressed as a sum of $|S(i)|^2$ up to k. The term $|S(0)|^2$ is a constant, ensuring that $D(0) = 0$. α_1 is a constant that controls the effective length of the SS signal to be T ($1 \leqq T \leqq L$). It satisfies

$$D(L/2) = \alpha_1 \cdot \left\{ \sum_{i=0}^{L/2} |S(i)|^2 - |S(0)|^2 \right\} = T. \tag{11}$$

Therefore,

$$\alpha_1 = T \Bigg/ \left\{ \sum_{i=0}^{L/2} |S(i)|^2 - |S(0)|^2 \right\}. \tag{12}$$

Then, by integrating $D(k)$ with respect to angular frequency $2\pi k/L$, the phase characteristic can be obtained as

$$\phi(k) = \frac{2\pi}{L} \cdot \sum_{i=0}^{k} D(i). \tag{13}$$

From this phase characteristic, the frequency spectrum of the SS signal, $S_s(k)$, is given by

$$S_S(k) = \begin{cases} |S(k)| \cdot \exp[-j\phi(k)] & (k = 0, 1, 2, \ldots, L/2) \\ S_S^*(L-k) & (k = L/2+1, \ldots, L-1) \end{cases} \tag{14}$$

Here, * represents the complex conjugate.

The waveform of the SS signal, $s_s(t)$, can be obtained by applying an inverse DFT to the frequency spectrum given by Eq. (14).

APPENDIX 2

PROOF OF SOME CHARACTERISTICS OF PROPOSED ALGORITHM

We prove that the SNR in the nth measurement becomes constant in the frequency band where a high SNR is obtained in the (n-1)th measurement and the estimate of SNR is given by C_n^2.

The proposed algorithm is summarized by equations Eqs. (9), (6), and (1), i.e.,

$$C_n^2 = \frac{E_s}{\sum_{k=0}^{L-1} \frac{P_N(k)}{\left|\hat{H}_{n-1}(k)\right|^2}} \tag{15}$$

$$|S_n(k)|^2 = C_n^2 \cdot \frac{P_N(k)}{\left|\hat{H}_{n-1}(k)\right|^2} \tag{16}$$

$$\hat{H}_n(k) = H(k) + \frac{N_n(k)}{S_n(k)}. \tag{17}$$

Here, n is the number of iterations. $N_n(k)(n = 1, 2, 3, \ldots)$ represents stationary noise added in the nth measurement, and its average is 0 as expressed by the following equations:

$$E[N_n(k)] = 0, \tag{18}$$

$$E[|N_n(k)|^2] = P_N(k). \tag{19}$$

The noise components included in the nth measurement result are $N_n(k)/S_n(k)$, as shown in Eq. (17), and their power spectrum is expressed using Eqs. (19) and (16).

$$E\left[\left|\frac{N_n(k)}{S_n(k)}\right|^2\right] = \frac{P_N(k)}{|S_n(k)|^2} = \frac{1}{C_n^2} \cdot \left|\hat{H}_{n-1}(k)\right|^2 \tag{20}$$

Then, the SNR in $\hat{H}_n(k)$ given by Eq. (17), i.e., $SNR_n(k)$, is expressed using Eq. (20) as

$$SNR_n(k) = \frac{|H(k)|^2}{E\left[\left|\frac{N_n(k)}{S_n(k)}\right|^2\right]} = C_n^2 \cdot \frac{|H(k)|^2}{\left|\hat{H}_{n-1}(k)\right|^2}. \tag{21}$$

When the SNR in the (n-1)th measurement result, $\hat{H}_{n-1}(k)$, is high for frequency k, we obtain

$$\begin{aligned} \left|\hat{H}_{n-1}(k)\right|^2 &= \left|H(k) + \frac{N_{n-1}(k)}{S_{n-1}(k)}\right|^2 \\ &\approx |H(k)|^2 . \end{aligned} \tag{22}$$

By substituting Eq. (22) into the denominator of Eq. (21), the SNR in $\hat{H}_n(k)$ for frequency k, at which the SNR in $\hat{H}_{n-1}(k)$ is high, is given by

$$SNR_n(k) \approx C_n^2, \text{(constant)}. \tag{23}$$

Thus, $SNR_n(k)$ is constant and independent of frequency, and C_n^2can be a good estimate of $SNR_n(k)$.

THE AUTHORS

Hirokazu Ochiai

Yutaka Kaneda

Hirokazu Ochiai was born in 1984. He studied information and communication engineering at Tokyo Denki University, Tokyo, Japan. He received a M.Eng. degree for the work of acoustic signal processing from the graduate school of engineering, Tokyo Denki University in 2011. He received the Student Presentation Award for his work about impulse response measurement from the Acoustical Society of Japan. He is currently working at Niigata Power Systems Co., Ltd.

●

Yutaka Kaneda was born in Osaka, Japan, in 1951. He received the B.E., M.E. and Doctor of Engineering degrees from Nagoya University, Nagoya, Japan, in 1975, 1977, and 1990 respectively. In 1977 he joined Nippon Telegraph and Telephone Corporation (NTT), Musashino, Tokyo, Japan, where he engaged in research on acoustic signal processing. In 2000 he joined Tokyo Denki University, Tokyo, Japan. He is currently a professor of acoustic signal processing at the Department of Information and Communication Engineering, Tokyo Denki University. His research interests include acoustical measurements, microphone array signal processing, and speech processing.

Dr. Kaneda is a member of the Acoustical Society of Japan, the Acoustical Society of America, Audio Engineering society, Institute of Electrical and Electronics Engineers, and the Institute of Electronics, Information and Communication Engineers of Japan.